

EFFECT OF UV-IRRADIATION TIME ON THE STRUCTURAL AND OPTICAL PROPERTIES OF POLYCRYSTALLINE OF 720 NM OF ZnSe FILM FOR OPTOELECTRONIC APPLICATIONS

M. H. ABDELJALIL^a, A. EL-TAHER^a, A. A. OTHMAN^b, G. A. M. ALI^c,
E. S. YOUSEF^{d,e}, E. R. SHAABAN^{a,*}

^aPhysics Department, Faculty of Science, Al-Azhar University, Assiut 71524,
Egypt

^bPhysics Department, Faculty of Science, Assiut University, Assiut, Egypt

^cChemistry Department, Faculty of Science, Al-Azhar University, Assiut 71524,
Egypt

^dPhysics Department, Faculty of Science, King Khalid University, P.O. Box 9004,
Abha, Saudi Arabia

^eResearch Center for Advanced Materials Science (RCAMS), King Khalid
University, Abha 61413, P.O. Box 9004, Saudi Arabia

Polycrystalline ZnSe thin films with thickness 720 nm were prepared by thermal evaporation under ultra vacuum onto glass substrates. The optical properties of the as deposited and UV-irradiated films with different exposure times (0, 30, 60, 90, and 120 min.) were reported. The polycrystalline nature of the films was detected by XRD measurements. XRD patterns for UV irradiated films show that the intensities of the peaks increase with increasing the UV-irradiated time but the full width at half maximum (FWHM) decreases. The optical constants of the films were calculated by Swanepoel's method in terms of wedge shape model to obtain both thickness and refractive index with high precision. The energy gap of ZnSe films was determined by using the transmission in terms of transmission spectra in the strong absorption region. In terms of the obtained results, the increase of exposure time improved shrinkage of non-uniform transmission in both the strong and medium absorption region of ZnSe film. The optimal improvement was at UV-irradiation time equal 120 min. Accordingly, the possibility of asserting that such tenability in the optical refractive index and energy gap of ZnSe thin films with UV-irradiation serves as a promising film in optoelectronic devices.

(Received April 4, 2020; Accepted July 15, 2020)

Keywords: Thin film; UV irradiated; XRD; Energy gap; Refractive index.

1. Introduction

Zinc selenide (ZnSe) is an attractive of II-VI Semiconductor compounds because of their specific optoelectronic device applications [1]. So, studying the optical properties of ZnSe over a wide wavelength range is very important. The technology of thin films is very important for fabricating and developing the need for the integrated circuit industry [2]. The requirement for the development of the smallest devices with higher speed especially in the new generation of integrated circuits requires advanced materials and new processing techniques suitable for future Giga scale integration (GSI) technology [3, 4]. So, the physics and technology of thin films play an important role to verify this target. Some of the important applications of thin films are microelectronics, communication, optical electronics, catalysis, coating of all kinds, and energy generation and conservation strategies. ZnSe thin films have a great number of applications in optical device technologies (solar cells, blue light-emitting devices, photodetectors, etc.). Moreover, a great portion of the mentioned devices can be fabricated in terms of thin-film technology these methods include thermal evaporation under vacuum, pulsed-laser deposition, molecular beam epitaxy, electrodeposition, and spray pyrolysis [5-8]. Moreover, the studying of

* Corresponding author: physicimohamed@gmail.com

the structural and optical properties of ZnSe thin film gives valuable information about the ZnSe properties. A lot of publications have been determined both the refractive index and thickness of thin films in terms of double beam spectrophotometer and optical spectroscopic ellipsometry (OSE). Both of the two techniques are very important to investigate the optical response of materials [9-13]. Radiation and its various sources improve many properties of crystalline materials in particular, as it adjusts and improves the structural properties and optical crystallization and improves the rate of electron transport between the energy levels of the amorphous materials, which makes them the transition to the crystalline phase, not to mention its ability to convert it to behave as approximates the mineral behavior in most cases. [14, 15]. Radiation also plays with its various sources role of the controlling local atomic changes for most of the substances subject to radiation [15-17]. Generally, significant changes in both linear and non-linear optical constants and parameters are mainly linked to radiation effect or on the other words related to irradiative stimulation if this expression is correct [18-19]. In this regard, absorption-edge transmits or its shifts as photo-darkening or photo-bleaching warrants the use of these materials in the main manufacture of a great number of optical tools [20-23]. Based on what has been mentioned, the precise identification of constants and optical parameters is very important, and this importance is not limited to knowledge of the basic mechanisms resulting from all these effects but extends to the use of these materials in modern technology. As to the method which utilizes to determine the optical constants and parameters of thin films that linked to it, one must consider that, in case of the optical thickness of the thin film is enough to create sundry interference extremes, it is possible to compute both of the refractive index and film thickness with high precision [8-16].

In the present framework, we will mainly look at starting with the analysis of Swanepoel's method in terms of wedge shape model [23] in the study of optical properties for as-deposited and UV treated ZnSe thin films in the time range between 0 and 120 minutes. This method based on the extremes of the interference fringes of the transmission spectrum for determination both film thickness and refractive index. The absorption coefficient and the energy gap have been determined in terms of transmission spectra in the high absorption region. Also, the present framework was concentrated fundamentally on all these properties, which are surely those that demand a much more itemized computation method in the present explanation which are the most rarely found in the literature.

2. Experimental

High purity ZnSe powder (99.999 %) from Aldrich Company was used for the preparation of ZnSe thin films with different thicknesses onto ultrasonically cleaned glass substrate kept at constant temperature (373 K) using a thermal evaporation unit (Denton Vacuum DV 502 A) under the vacuum of 10^{-6} Pa. To obtain the optimal conditions for a homogeneous thin film, a mechanical rotation of the substrate holder (≈ 30 rpm) during deposition was used. Both the film thickness and the deposition rate were controlled using a quartz crystal monitor DTM 100. The deposition rate was kept at 2 nm/s during the preparation of thin films. Both the structure of the powder and thin films were examined by X-ray diffraction (XRD) (Philips X-ray diffractometry (1710)) with Ni-filtered CuK_α radiation with ($\lambda = 0.15418$ nm). Both the morphology the elemental composition of the ZnSe thin films were analyzed by using energy dispersive X-ray spectrometer unit (EDXS) interfaced with a scanning electron microscope, SEM (JOEL XL) operating an accelerating voltage of 30 kV. The relative error of determining the indicated elements does not exceed 2 %. Illumination of the studied films was carried out at 300 K using UV lamp (Minera-light, San Gabriel, CA) with 20 mW/cm^2 and infrared cut filter, to suppress any temperature effect on the absorption edge shift. The UV exposure time was taken as UV-irradiated films with different exposure times (0, 30, 60, 90, and 120 min.). The measurements of the transmittance, T was carried out in terms of a double-beam spectrophotometer (Jasco V670) at normal incidence of light in a wavelength (λ) range between 400 and 2500 nm. The measured transmittance spectrum was carried out without a glass substrate in the reference beam to calculate the refractive index and the film thickness of ZnSe thin films according to Swanepoel's method.

3. Theoretical foresight

In terms of Swanipoel relationship, the transmission of thin films of uniform thickness, d and their complex refractive index, \tilde{n} which equaled to $\tilde{n} = n - ik$ and α refers to on absorption coefficient can be expressed as follows [25, 27, 28]:

$$T(\lambda, s, n, d, k) \Big|_{k=0} = \frac{Ax}{B - Cx \cos(\varphi) + Dx^2} \quad (1)$$

It should be noted that the interference is done through three media that have different refractive indexes, which are air, that has a refractive index equal to the correct one, namely $n_o = 1$ and also a refractive index for the glass substrate, s and finally a refractive index for the studied thin films, n .

$$\text{Here, } A = 16n^2s, \quad B = (n+1)^3(n+s^2), \quad C = 2(n^2-1)(n^2-s^2), \\ D = (n-1)^3(n-s^2), \quad \varphi = 4\pi d / \lambda, \quad x = \exp(-\alpha d) \text{ and } k = \frac{\alpha\lambda}{4\pi}.$$

All parameters in these equations are as a function of wavelength. It is not complex to view that at $\cos(\varphi) = \pm 1$, that is, one can reformulate the first equation (Eq. 1) at the extremes of the interference points as follows:

$$T_{Mo} = \frac{Ax}{B - Cx + Dx^2} \text{ for (the interference maxima)} \quad (2)$$

and

$$T_{mo} = \frac{Ax}{B + Cx + Dx^2} \text{ for (the interference minima)} \quad (3)$$

Schematically, the expression about non-uniform thin films has been illustrated in Fig. 1.

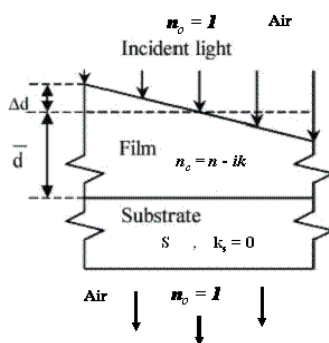


Fig. 1. Modelled sample structure of a non-uniformly thick, absorbing thin film on a transparent substrate.

This figure is presumed that the thickness changes linearly through the illuminated area [29, 30], thus it can be illustrated by: $d = \bar{d} \pm \Delta d$, Δd refers to the actual changes in thickness from the average thickness \bar{d} , as appeared in Fig. 1, and must not be confounded with a standard deviation of computed values, RMSE. Deviation utilized by other workers [25]:

$$RMSE = \sqrt{\frac{\sum_{i=1}^q (d - (\bar{d}))^2}{q}} \quad (4)$$

Here, the interference style shrinks dramatically on account of the thickness is not uniform. Now, Eq. (1) must be integrated over both the thickness of the film, Δd and x for it to more exactly depict the transmission spectrum $T_{\Delta d}(\lambda)$ [26]. The transmittance then becomes as follows:

$$T_{\Delta d} = \frac{1}{\varphi_2 - \varphi_1} \int_{\varphi_1}^{\varphi_2} \frac{A\bar{x}}{B - C\bar{x} \cos \varphi + D\bar{x}^2} d\varphi \quad (5)$$

Here, $\varphi_1 = 4\pi n(\bar{d} - \Delta d) / \lambda$, $\varphi_2 = 4\pi n(\bar{d} + \Delta d) / \lambda$ and $\bar{x} = \exp(-\alpha \bar{d})$.

The integral yields:

$$T_{\Delta d} = \frac{\lambda}{4\pi n \Delta d} \frac{a}{(1-b^2)^{1/2}} \left[\tan^{-1} \left(\frac{1+b}{(1-b^2)^{1/2}} \tan \frac{\varphi_2}{2} \right) - \tan^{-1} \left(\frac{1+b}{(1-b^2)^{1/2}} \tan \frac{\varphi_1}{2} \right) \right] \quad (6)$$

Here,

$$a = \frac{A\bar{x}}{B + D\bar{x}^2} \quad \text{and} \quad b = \frac{C\bar{x}}{B + D\bar{x}^2} \quad (7)$$

As a result one will have:

$$\text{Maxima:} \quad T_{M\bar{x}} = \frac{\lambda}{4\pi n \Delta d} \frac{a}{(1-b^2)^{1/2}} \left[\tan^{-1} \left(\frac{1+b}{(1-b^2)^{1/2}} \tan \frac{2\pi n \Delta d}{\lambda} \right) \right] \quad (8)$$

$$\text{Minima:} \quad T_{m\bar{x}} = \frac{\lambda}{4\pi n \Delta d} \frac{a}{(1-b^2)^{1/2}} \left[\tan^{-1} \left(\frac{1-b}{(1-b^2)^{1/2}} \tan \frac{2\pi n \Delta d}{\lambda} \right) \right] \quad (9)$$

Substituting: Eq. (7) in: Eqs. (8 & 9) and utilizing Eq. (5), the subsequence consolidated equations between the main experimental envelopes T_M and T_m of the non-uniform film and the envelopes T_{Mo} and T_{mo} of the uniform film, with a thickness equal to the average thickness of the non-uniform film, are obtained:

$$T_M = \frac{\sqrt{(T_{Mo} T_{mo})}}{\chi} \cdot \tan^{-1} \left[\sqrt{\left(\frac{T_{Mo}}{T_{mo}} \right)} \cdot \tan \chi \right] \quad (10)$$

$$T_m = \frac{\sqrt{(T_{Mo} T_{mo})}}{\chi} \cdot \tan^{-1} \left[\sqrt{\left(\frac{T_{mo}}{T_{Mo}} \right)} \cdot \tan \chi \right] \quad (11)$$

where

$$\chi = \frac{2\pi n \Delta d}{\lambda} \quad (12)$$

and

$$0 < \chi < \pi/2 \quad (\text{or equivalently, } 0 < \Delta d < \lambda/4n) \quad (13)$$

4. Results and discussion

4.1. The crystallographic structure of ZnSe thin films

Fig. 2 displays XRD diffractogram of ZnSe powder according to JCPDS Data file no.: 05-0566, it can be indexed to ZnSe cubic phase with polycrystalline. The XRD patterns of UV-irradiated ZnSe films with different exposure times (0, 30, 60, 90, and 120 min.) are shown in Fig. 2. The observed peaks of ZnSe thin films are compared with the standard JCPDS values, which showed that the films give a structure matching with (JCPDS file no.: 05-0566-cubic) zinc blend Cubic structure.

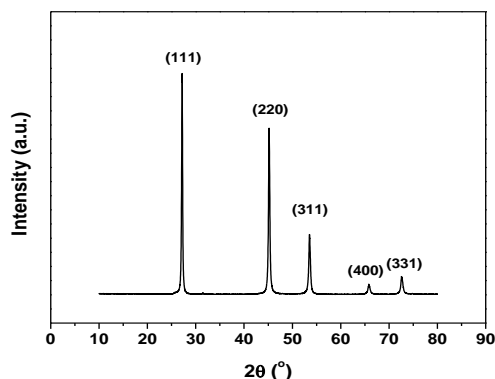


Fig. 2. XRD patterns of the powder of ZnSe.

The observed peaks of ZnSe films are polycrystalline with peaks detected at $2\theta = 28.56^\circ$, 47.52° and 56.29° corresponding to C(1 1 1), C(2 2 0) and C(3 1 1) orientations, respectively. Fig. 3 shows that the intensities of the peaks increase with increasing the UV-irradiated time but the full width at half maximum (FWHM) decreases with increasing the film thickness.

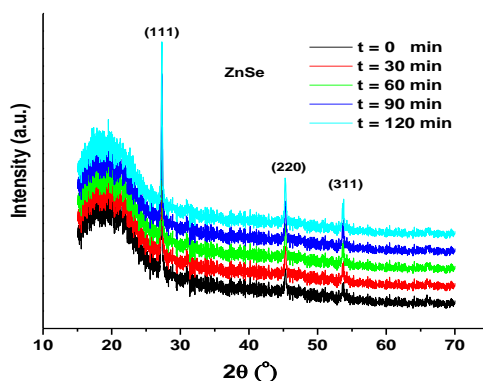


Fig. 3. X-ray patterns of as-obtained and UV treated ZnSe thin films.

4.2. Optical analysis

In a spectral range extended from 400 to 2500 nm, the experimental results presented in Fig. 4 shows the variation of transmission $T(\lambda)$ of ZnSe thin film as a function exposure time of UV-irradiation. As clearly observed in the transmission spectrum, distinct interference fringes are observed at a longer wavelength (transparent region) with a large intensity approaching $\approx 86\%$. As we move to a shorter wavelength where the absorption starts to take place within the film, the intensity of the interference fringes start to decrease gradually until it approached zero at the edge of the optical band gap of the deposited films. Also, shrinkage appears in transmission spectra in both weak and medium absorption regions that reflect the non-uniformity of the films. This

shrinkage has improved with the increasing exposure time of UV-irradiation as seen in Fig. 5. Fig. 6 shows a blue shift of transmission spectra with increasing UV-irradiation time ZnSe thin films.

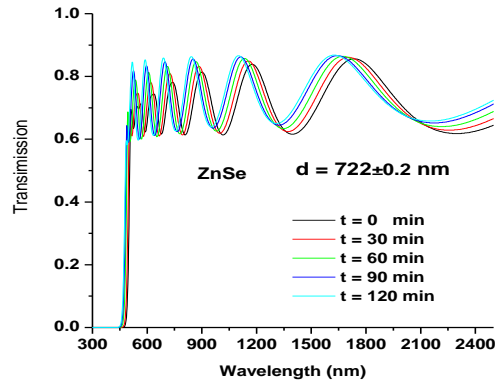


Fig. 4. Transmission spectra of as-obtained and UV treated ZnSe thin films.

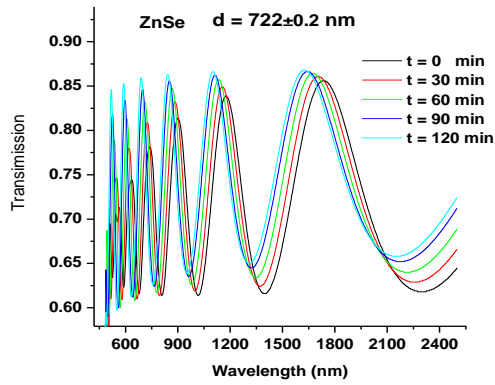


Fig. 5. Improvement of the shrinkage of transmission spectra with increasing UV-irradiation time ZnSe thin films.

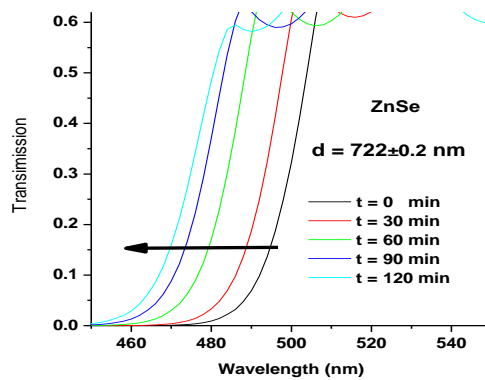


Fig. 6. Blue shift of transmission spectra with increasing UV-irradiation time ZnSe thin films.

The two relations (10 & 11) are independent transcendental in T_{Mo} , T_{mo} and $\chi \cdot T_{Mo} \equiv T_s$ in the transparent region as illustrated in Fig. 7. In order to compute T_{mo} and χ in mentioned spectral region, one can solve Eqs. (10, 11) utilizing an approximate solution to a system of nonlinear relations by *minerr* function in Mathcad 2000 program.

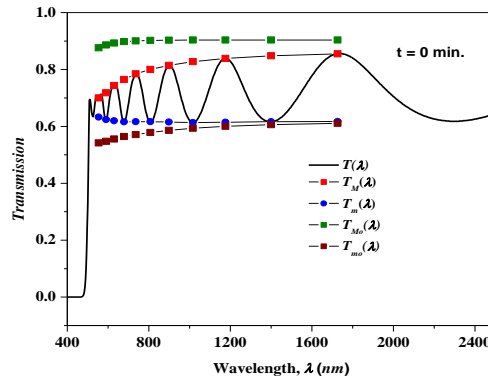


Fig. 7. Shrinkage of transmission spectrum in strong and medium absorption region of as deposited ZnSe film. The values of displayed T according to the text.

The fundamental relation for the interference fringe points starting from the long-wavelength will be written in accordance to previous papers [10, 15, 16] as follows:

$$\frac{l}{2} = \frac{2n\bar{d}}{\lambda} - m_1 \quad l = 0, 1, 2, 3, 4, \dots \tag{14}$$

Here: m_1 is the order number of the first at ($l = 0$) extreme considered, integer for a maximum or half integer for a minimum. Substituting Eq. (12) in Eq. (14) yields:

$$\frac{l}{2} = \left(\frac{\bar{d}}{\pi\Delta d} \right) \chi - m_1 \tag{15}$$

In case of plotted $\frac{l}{2}$ as a function of χ for the transparent region, the slope and m_1 , of Eq. (15) can be obtained as shown in Fig. 8 (for the first studied thin film). Eq. (15) can now be utilized to compute χ for the extrema in the absorption region, and T_{M_o} and T_{m_o} can be computed from Eqs. (10 & 11), as illustrated below.

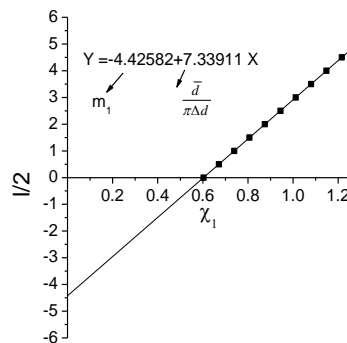


Fig. 8. Plot of $l/2$ against χ_1 , in order to determine χ for the as-obtained film as an example for the rest films.

Now T_{m_o} and χ are computed from Eqs. (10 & 11), utilizing the values of T_M and T_m at the extrema of each spectrum summarized in Table 1 and putting $T_{M_o}(\lambda) = T_s(\lambda)$. The values of

χ are shown as χ_1 , in Table 1, and $\frac{l}{2}$ is plotted as a function of χ , according to Eq. (15) in Fig. 8.

Table 1. Values of λ , T_M and T_m for the five different UV irradiation time of ZnSe thin film corresponding to transmission spectra. The calculated values of refractive index and film thickness are based on the wedge shape model.

t = 0 min.													
λ	s	T_M	T_m	χ_1	X	T_{M_0}	T_{m_0}	n_1	$d_1(\text{nm})$	m_0	m	$d_2(\text{nm})$	n_2
554	1.517	0.6998	0.6324	1.325	1.284	0.8764	0.5416	2.677	----	6.993	7	719.5	2.677
590	1.487	0.7182	0.6242	1.242	1.216	0.8862	0.5474	2.647	696	6.47	6.5	722.1	2.647
630	1.466	0.7434	0.6194	1.142	1.148	0.893	0.5556	2.609	707.3	5.961	6	723.6	2.609
678	1.452	0.7648	0.6162	1.059	1.08	0.8977	0.564	2.574	715.4	5.454	5.5	724.9	2.574
736	1.44	0.7843	0.6163	0.985	1.012	0.9007	0.5713	2.54	721.3	4.956	5	725.3	2.54
808	1.432	0.8003	0.6165	0.92	0.944	0.9024	0.5785	2.51	727.2	4.457	4.5	725.7	2.51
898	1.431	0.8145	0.6154	0.856	0.875	0.9031	0.5861	2.48	728	3.967	4	724.8	2.48
1016	1.431	0.8273	0.6137	0.792	0.807	0.9034	0.5937	2.455	718.2	3.47	3.5	725.1	2.455
1176	1.428	0.8389	0.6148	0.736	0.739	0.9035	0.6002	2.435	721.1	2.967	3	727	2.435
1400	1.429	0.8482	0.6167	0.689	0.671	0.9035	0.6059	2.416	735.2	2.473	2.5	726.7	2.416
1726	1.425	0.8552	0.617	0.649	0.603	0.9035	0.6107	2.383	----	1.989	2	722.9	2.383
$\bar{d}_1 = 719 \text{ nm} \quad \sigma_1 = 11.7 \text{ nm (1.53 \%)} \quad \bar{d}_2 = 724 \text{ nm} \quad \sigma_2 = 2.2 \text{ nm (0.3 \%)}$													
t = 60 min.													
s	T_M	T_m	χ_1	X	T_{M_0}	T_{m_0}	n_1	$d_1(\text{nm})$	m_0	m	$d_2(\text{nm})$	n_2	
518	1.563	0.8423	0.5951	0.993	1.048	0.8612	0.5884	2.516	----	6.968	7	715.1	2.516
550	1.521	0.8472	0.5978	0.949	0.993	0.8751	0.5932	2.481	702.9	6.469	6.5	715.3	2.481
588	1.488	0.8499	0.6041	0.918	0.938	0.8858	0.6	2.448	694.7	5.956	6	717.2	2.448
634	1.465	0.854	0.6118	0.856	0.883	0.8935	0.6068	2.42	709	5.445	5.5	719.2	2.42
688	1.447	0.8577	0.62	0.788	0.828	0.8984	0.6131	2.387	711	4.951	5	718.9	2.387
756	1.432	0.8592	0.6276	0.749	0.773	0.9013	0.62	2.361	695.1	4.443	4.5	721	2.361
844	1.43	0.8603	0.6329	0.71	0.718	0.9028	0.6295	2.343	706.8	3.927	4	725.1	2.343
952	1.429	0.8616	0.638	0.666	0.663	0.9033	0.6385	2.312	729.9	3.436	3.5	725.2	2.312
1100	1.431	0.863	0.6439	0.622	0.609	0.9035	0.6444	2.29	728.5	2.952	3	723.5	2.29
1310	1.428	0.8652	0.6494	0.588	0.554	0.9035	0.6492	2.273	729.4	2.459	2.5	723.9	2.273
1622	1.431	0.8686	0.654	0.562	0.499	0.9035	0.6535	2.251	----	1.976	2	720.6	2.251
$\bar{d}_1 = 712 \text{ nm} \quad \sigma_1 = 14.1 \text{ nm (1.98 \%)} \quad \bar{d}_2 = 720 \text{ nm} \quad \sigma_2 = 3.7 \text{ nm (0.5 \%)}$													
t = 120 min.													
λ	s	T_M	T_m	χ_1	X	T_{M_0}	T_{m_0}	n_1	$d_1(\text{nm})$	m_0	m	$d_2(\text{nm})$	n_2
534	1.541	0.7876	0.5997	0.852	0.984	0.8688	0.5631	2.587	----	6.969	7	712.9	2.587
568	1.503	0.8021	0.6013	0.821	0.937	0.8808	0.5686	2.555	669.3	6.454	6.5	714.8	2.555
608	1.476	0.8113	0.6047	0.81	0.89	0.8897	0.5787	2.525	669.4	5.909	6	720.7	2.525
654	1.458	0.8226	0.6088	0.781	0.843	0.8957	0.5887	2.49	705	5.394	5.5	723.7	2.49
710	1.443	0.8326	0.6131	0.751	0.796	0.8996	0.5955	2.457	717.1	4.902	5	723.9	2.457
780	1.432	0.8391	0.6176	0.733	0.749	0.9019	0.602	2.429	712.4	4.404	4.5	725.2	2.429
870	1.434	0.8444	0.6224	0.717	0.703	0.903	0.6099	2.409	722	3.906	4	726.9	2.409
982	1.425	0.8503	0.6269	0.693	0.656	0.9034	0.6177	2.379	730.4	3.421	3.5	726.1	2.379
1134	1.428	0.8556	0.6297	0.667	0.609	0.9035	0.6244	2.355	727.1	2.934	3	725.7	2.355
1350	1.429	0.8596	0.6324	0.646	0.562	0.9035	0.6304	2.336	734.8	2.445	2.5	725.7	2.336
1666	1.428	0.8625	0.6361	0.634	0.515	0.9035	0.6346	2.306	----	1.968	2	721.2	2.306
$\bar{d}_1 = 710 \text{ nm} \quad \sigma_1 = 24.6 \text{ nm (3.5 \%)} \quad \bar{d}_2 = 722 \text{ nm} \quad \sigma_2 = 4.7 \text{ nm (0.65 \%)}$													

Next, the best straight lines through the points of the transparent region are drawn. The deviation of the points for larger χ , from these straight lines indicates the onset of absorption, and these points must be rejected. From Fig. 8 (for the first studied film, as an example), and Eq. (15) can be represented by the following expressions for the last four studied films, respectively:

$$l/2 = 7.339\chi - 4.425 \quad (16)$$

$$l/2 = 9.70\chi - 5.617 \quad (17)$$

$$l/2 = 10.68\chi - 5.505 \quad (18)$$

$$l/2 = 9.31\chi - 4.902 \quad (19)$$

$$l/2 = 9.11\chi - 4.545 \quad (20)$$

The value of χ at each extreme is now computed from the expressions which result from modifying these last four equations. The new values of χ are shown in Table 1. Using these values of χ , together with the values of T_M and T_m , the T_{Mo} and T_{mo} are computed from Eqs. (10 & 11). These values of T_{Mo} and T_{mo} are shown in Table 1.

The obtained values of T_{Mo} and T_{mo} can now be utilized to derive: \bar{d} , Δd and $n(\lambda)$ via the method for uniform films, discussed in detail in our previous works [29, 30]. We shall now briefly discuss this method.

Also, the values of n_1 can be used to derive d_2 from the basic equation for the interference fringes, $2n\bar{d} = m\lambda$ (m is the order number of the interference extrema), and also improved values for n , shown as n_2 , as described in detail previously [32-34]. Fig. 9 illustrates the dependence of n on wavelength for different exposure times (0, 30, 60, 90, and 120 min.) of UV-irradiated of ZnSe films. This figure shows that the refractive index, n_2 decreases with increasing exposure times, over the entire spectral range studied.

Following Swanepoel [25] recommends, in the case of uniform films, that the T_{Mo} curve be utilized over all spectrum range, namely, strong, medium, and weak absorption regions. The corresponding expression to compute the absorbance, x is as follows:

$$x = \frac{E_{Mo} - [E_{Mo}^2 - (n^2 - 1)^3(n^2 - s^4)]^{1/2}}{(n - 1)^3(n - s^2)}, \quad \alpha = -\frac{1}{d} \times \ln(x) \quad (21)$$

where $E_{Mo} = \frac{8n^2s}{T_{Mo}} + (n^2 - 1)(n^2 - s^2)$. $\alpha(\lambda)$ is then computed, utilizing the main expression $\alpha = -\frac{1}{d} \times \ln(x)$. The absorption coefficients, α of the studied thin films depending on the wavelength, λ in the regions of their transparency $\lambda > 500(\text{nm})$ were also computed utilizing the subsequence relation [35-37]:

$$\alpha(\lambda) = \frac{1}{d} [\ln(1 - R_1) + \ln(1 - R_2) + \ln(1 - R_{12}) - \ln(T(\lambda))] \quad (22)$$

On the other word, based on [35], the absorption in the ranging from 300 to 500 nm is almost characterized by the all met conditions: strong absorption in the film, transparency of substrate, and satisfied inequality $n^2 \gg k^2$ and thus according to [25, 37], one can express about absorption coefficient in the mentioned range by the following equation:

$$\alpha(\lambda) = \frac{1}{d} [\ln(1 - R_1) + \ln(1 - R_2) + \ln(1 - R_{12}) - \ln(T(\lambda))] \quad (23)$$

Here: $T(\lambda)$ is the transmittance of the film at the selected λ and parameters R_1, R_{12}, R_2 reflection coefficients from the following boundaries:

Air_film:

$$R_1 = \left(\frac{n(\lambda)-1}{n(\lambda)+1} \right)^2 \quad (24)$$

Substrate_air:

$$R_{12} = \left(\frac{1-s(\lambda)}{1+s(\lambda)} \right)^2 \quad (25)$$

Film_substrate:

$$R_2 = \left(\frac{s(\lambda)-n(\lambda)}{s(\lambda)+n(\lambda)} \right)^2 \quad (26)$$

Fig. 9 shows the dependence of the refractive index n on the incident photon energy ($h\nu$) for different exposure times (0, 30, 60, 90, and 120 min.) of UV-irradiated ZnSe films.

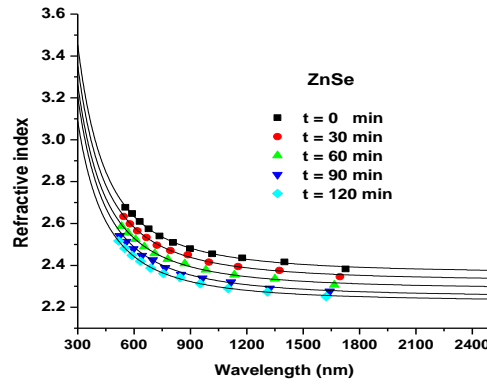


Fig. 9. The spectral dependence of refractive index, n for the studied films.

It is well known that in the near of the absorption edge, for allowed direct band-to-band transitions, the absorption coefficient is described in terms of the following relationship

$$\alpha(h\nu) = \frac{K (h\nu - E_g^{opt})^m}{h\nu} \quad (27)$$

where K is the edge width parameter independent of photon energy for respective transitions [38], E_g^{opt} is the optical energy gap and m is a number which characterizes the transition process. various authors [29-31] have suggested different values of m for different glasses, $m= 2$ for most amorphous semiconductors (indirect transition), and $m =1/2$ for most of the crystalline semiconductor (direct transition). In the case of polycrystalline of ZnSe thin films with exposure time, the direct transition was valid.

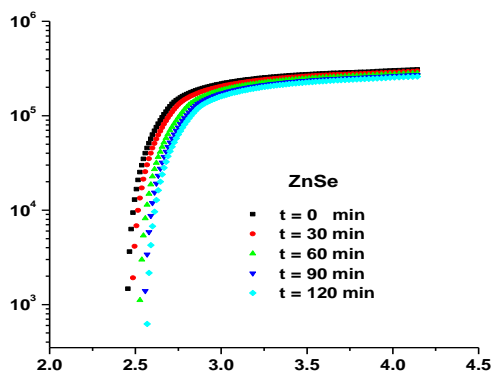


Fig. 10. The dependence of the absorption coefficient, α on the incident photon energy ($h\nu$) for the studied films.

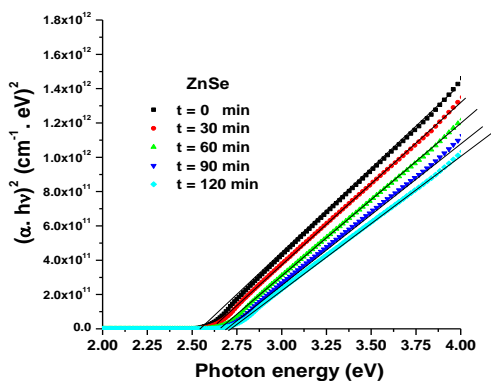


Fig. 11. The dependence of the absorption coefficient, α on the incident photon energy ($h\nu$) for the studied films.

Fig. 11 shows the plots of $(\alpha h\nu)^2$ versus photon energy ($h\nu$) for an exposure time of UV-irradiation for ZnSe thin films. The optical energy gap can be obtained by the extrapolation at the linear part in the $(\alpha h\nu)^2$ versus ($h\nu$) at $(\alpha h\nu)^2 = 0$ for the allowed direct transition. The direct energy gap increases from 2.55 to 2.70 eV with an increased exposure time of UV-irradiated of ZnSe films.

5. Conclusions

Polycrystalline ZnSe thin films with thickness 720 nm were prepared by thermal evaporation under ultra vacuum onto glass substrates. XRD patterns for UV irradiated films show that the intensities of the peaks increase with increasing the UV-irradiated time but the full width at half maximum (FWHM) decreases. The effect of increasing UV-irradiation time on optical constants and energy gap of the ZnSe films were investigated. The optical constants of the films were calculated by Swanepoel's method in terms of wedge shape model to obtain both thickness and refractive index with high precision. The energy gap of ZnSe films was determined by using the transmission in the strong absorption region that increases with increasing UV-irradiation time.

In terms of the obtained results, the increase of exposure time improved shrinkage of non-uniform transmission in both strong and medium absorption region and convert it to uniform transmission at optimal UV-irradiation time equal 120 min. Accordingly, the possibility of asserting that such tuneability in optical refractive index and energy gap of ZnSe thin films with UV-irradiation serves as a promising film in optoelectronic devices.

Acknowledgments

The authors extend their appreciation to the Deanship of Scientific Research at King Khalid University for funding this work through a research project under grant number (G.R.P./55/40).

References

- [1] J. J. Zhu, Y. Kolytyn, A. Gedanken, *Chem. Mater.* **12**(1), 73 (2000).
- [2] L. Eckertová, *Physics of Thin Films*, Springer Science & Business Media (2012).
- [3] M. P. Valkonen, S. Lindroos, M. Leskela, *Appl. Surf. Sci.* **134**, 283 (1998).
- [4] I. T. Sinaoui, F. Chaffar Akkar, F. Aousgi, M. Kanzari, *Int. J. Thin Fil. Sci. Tec.* **3**(1), 19 (2014).
- [5] E. R. Shaaban, M. Abdel-Rahman, El Sayed Yousef, M. T. Dessouky, *Thin Solid Films* **515**, 3810 (2007).
- [6] Y. P. Venkata Subbaiah, P. Prathap, M. Devika, K. T. R. Reddy, *Physica B*: **365**, 240 (2005).
- [7] S. Lalitha, R. Sathyamoorthy, S. Senthilarasu, A. Subbarayan, K. Natarajan, *Solar Energy Materials & Solar Cells* **82**, 187 (2004).
- [8] Y. Ni, G. Yin, J. Hong, Z. Xu, *Mater. Res. Bull.* **39**, 1967 (2004).
- [9] S. Zhao, F. Ma, Z. Song, *Optical Materials* **30**, 910 (2008).
- [10] K. Luo, S. Zhou, L. Wu, *Thin solid films* **517**, 5974 (2009).
- [11] P. Eiamchai, P. Chindaudom, A. Pokaipisit, P. Limsuwan, *Current Applied Physics* **9**, 707 (2009).
- [12] J. Park, J. Kook, Y. Kang, *Bull. Korean Chem. Soc.* **31**, 397 (2010).
- [13] N. Khemiri, B. Khalfallah, D. Abdelkader, M. Kanzari, *Int. J. Thin Fil. Sci. Tec.* **3**(1), 7 (2014).
- [14] E. R. Shaaban, M. A. Kaid, M. G. S. Ali, *Journal of Alloys and Compounds* **613**, 324 (2014).
- [15] E. R. Shaaban, Y. A. M. Ismail, H. S. Hassan, *Journal of Non-Crystalline Solids* **376**, 61 (2013).
- [16] D. Prakash, A. M. Aboaraia, M. El-Hagary, E. R. Shaaban, K. D. Verma, *Ceramics International* **42**, 2676 (2016).
- [17] S. R. Elliott, *Physics of Amorphous Materials*, Longman, New York (1990).
- [18] P. J. S. Ewen, A. E. Owen. *High-performance glasses*, Blackie, London, 287 (1992).
- [19] E. Márquez, J. B. Ramirez-Malo, J. Fernandez-Pena, P. Villares, R. Jiménez-Garay, P. J. S. Ewen, A. E. Owen, *J. Non-Cryst. Solids* **164-166**, 1223 (1993).
- [20] E. R. Shaaban, M. S. Abd El-Sadek, M. El-Hagary, I. S. Yahia, *Physica Scripta* **86**, 015702 (2012).
- [21] El S. Yousef, A. El-Adawy, N. El Koshkhany, E. R. Shaaban, *Journal of Physics and Chemistry of Solids* **67**, 1649 (2006).
- [22] S. H. Mohamed, E. R. Shaaban, *Physica B: Condensed Matter* **406**, 4327 (2011).
- [23] Z. Cimpric, F. Kosek. *Physica Status Solidi A* **93**(1), K55 (1986).
- [24] D. Minkov et al., *Journal of Non-Crystalline Solids* **90**(1-3), 481 (1987).
- [25] R. Swanepoel, *Journal of Physics E: Scientific Instruments* **16**(12), 1214 (1983).
- [26] J. C. Manifacier, J. Gasiot, J. P. Fillard. *Journal of Physics E: Scientific Instruments* **9**(11), 1002 (1976).
- [27] E. R. Shaaban, *Materials chemistry and physics* **100**(2-3), 411 (2006).
- [28] E. R. Shaaban, M. Abdel-Rahman, El Sayed Yousef, M. T. Dessouky. *Thin Solid Films* **515**, 7 (2007).
- [29] E. Marquez, J. B. Ramirez-Malo, J. Fernandez-Pea, R. Jiménez-Garay, P. J. S. Ewen, A. E. Owen, *Opt. Mater.* **2**, 143 (1993).
- [30] E. R. Shaaban, *Philosophical Magazine* **88**, 781 (2008).
- [31] R. Swanepoel, *J. Phys. E* **17**, 896 (1984).

- [32] E. Márquez, J. M. González-Leal, A. M. Bernal-Oliva, R. Jiménez-Garay, T. Wagner, J. Non-Cryst. Solids **354**, 503 (2008).
- [33] M. El-Hagary, M. Emam-Ismail, E. R. Shaaban, S. Althoyaib, Mater. Chem. Phys. **132**, 581 (2012).
- [34] E. R. Shaaban, Ishu Kansal, S. H. Mohamed, J. M. F. Ferreira, Physica B: **404**, 3571 (2009).
- [35] J. I. Pankove, Optical Processes in Semiconductors (Dover Publications, New York, 1975).
- [36] E. R. Shaaban, N. Afify, A. El-Taher, Journal of Alloys and Compounds **482**(1-2), 400 (2009).
- [37] V. V. Brus, Z. D. Kovalyuk, P. D. Maryanchuk. Technical Physics **57**(8), 1148 (2012).
- [38] M. Nowak, Thin Solid Films **266**, 258 (1995).
- [39] J. I. Pankove, Optical Processes in Semiconductors, Dover, New York, 44 (1971).
- [40] E. A. Davis, N. F. Mott, Philos. Mag. **22**, 903 (1970).
- [41] E. R. Shaaban, Appl. Phys. A **115**, 919 (2014).